Frequency-difference imaging for multi-frequency complex-valued ECT

Citation for published version:
Wang, H, Zhang, M & Yang, Y 2020, Frequency-difference imaging for multi-frequency complex-valued ECT. in *2019 IEEE International Conference on Imaging Systems and Techniques (IST).* IEEE, 2019 IEEE International Conference on Imaging Systems and Techniques , ABU DHABI, United Arab Emirates, 8/12/19. https://doi.org/10.1109/IST48021.2019.9010531

Digital Object Identifier (DOI):
10.1109/IST48021.2019.9010531

Link:
Link to publication record in Edinburgh Research Explorer

Document Version:
Peer reviewed version

Published In:
2019 IEEE International Conference on Imaging Systems and Techniques (IST)

Frequency-difference imaging for multi-frequency complex-valued ECT

Haokun Wang*
School of Engineering
University of Edinburgh
Edinburgh, UK
Haokun.Wang@ed.ac.uk

Maomao Zhang*
Shenzhen LeEngStar Technology Co.,Ltd
Shenzhen, China
zhangmaomao@leengstar.com

Yunjie Yang
School of Engineering
University of Edinburgh
Edinburgh, UK
y.yang@ed.ac.uk

***Abstract*—Complex-valued Electrical Capacitance Tomography (CVECT) system with multi-frequency excitation scheme has been implemented in recent studies for imaging both conductivity and permittivity components, where time-difference (TD) imaging method was employed. This paper explores the feasibility of performing frequency-difference (FD) imaging of CVECT using Multiple Measurement Vector (MMV) model. Experiments based on simulation data were performed to evaluate the proposed framework. Comparison with conventional Tikhonov regularization algorithm was presented. The results confirm that it is feasible to perform FD imaging with multi-frequency CVECT system, and MMV outperforms conventional image reconstruction algorithms in terms of image quality and efficiency.**

***Index Terms*—Complex-valued ECT (CVECT), multi-frequency, frequency-difference imaging, multiple measurement vector model.**

I. Introduction

Electrical Capacitance Tomography (ECT) is a non-invasive and non-intrusive imaging technology that can achieve the reconstruction of permittivity distribution of dielectric materials [1]. Among various industrial process tomography modalities, ECT has extensive applications because its unique sensing principle making it be able to scan objects without directly contact with the testing materials. Normally, the changes of concentration and/or distribution of the permittivity of the material can cause the changes of capacitance between pairs of electrodes. Meanwhile, changes of conductivity of the material are usually negligible. However, in oil and gas industry, the application of typical ECT in multiphase flow measurement is immensely restricted by the water content, due to the ECT measurement being sensitive to high background conductivity [2]. A number of studies suggest the use of ECT and Electrical Resistance Tomography (ERT) dual-modality technique as a supplementary method to deal with multiphase flow measurement involving highly conductive substances [3]. However, direct electrode contact with measuring object in ERT brings risks in practical applications. Corrosion or sediment on electrode surfaces can cause system failures in long-term measurement process.

*Note that Haokun Wang and Maomao Zhang contributed equally to this work.

To achieve the goal of accurate, non-invasive detecting a wide range of permittivity and conductivity distribution within a certain spatial area, several studies have attempted to extend the capacity of conventional tomography modalities. For instance, Capacitively Coupled Electrical Resistance Tomography (CCERT) technique as a combination of Capacitively Coupled Contactless Conductivity Detection (C^4D) and ERT techniques has been reported recently [4]. The changes of conductivity distribution can be detected by CCERT system by using a capacitive sensor. In this way, the characteristic of C^4D technique enables CCERT to non-intrusively perform the measurement. Additionally, compared with ERT, the implementation of CCERT is more simpler, which is also a negligible factor in industry applications. In addition to CCERT, Zhang et al. [5] proposed an extended complex-valued ECT (CVECT) model for simultaneous imaging of permittivity and conductivity components by using time-difference (TD) method. The improved ECT model was validated by simulation data, showing it to be able to measure complex permittivity distribution by using conventional ECT sensors. All these pioneering work has demonstrated great potential to tackle the measurement challenge of highly conductive objects by using capacitive sensor. Meanwhile, CVECT model also explores the use of multi-frequency excitation to obtain extra information or better image quality.

However, existing work was mainly focused on the image reconstruction problem of multi-frequency measurement under time difference setup and used Tikhonov regularization algorithm and simulation data only. Therefore, the quality and efficiency of the reconstructed images and reconstruction process are not ideal.

In this paper, the feasibility of performing frequency-difference (FD) imaging of CVECT using multi-frequency excitation was studied. Simultaneous reconstruction of multi-frequency conductivity and permittivity distribution was realized by introducing the Multiple Measurement Vector (MMV) model. The correlation of FD images were utilized as a priori information to improve image quality and the Alternating Direction Method of Multipliers (ADMM) was adopted to solve the MMV problem. The performance of the proposed method was evaluated by numerical experiments and image reconstruction using Tikhonov Regularization was presented to benchmark the new method.

II. MMV Based Frequency-Difference Imaging

A. Principle of ECT

For a typical ECT system, the forward problem describes the relationship between the measured capacitance from the pairs of electrodes and the permittivity distribution within the detecting region. It can be expressed by the following equation [1]:

$$C = \frac{Q}{V} = -(\frac{1}{V}) \oint_{\Gamma} \varepsilon(x, y) \cdot \nabla\phi(x, y) d\Gamma \tag{1}$$

where V is the potential difference between two electrodes sensors, $\varepsilon(x, y)$ is the permittivity distribution within the detecting region, $\phi(x, y)$ is the potential distribution, $\nabla$is the gradient operator and Γ is the electrode surface.

Equation (1) can be linearized into (2), the linearised relationship between the measured capacitance and the calculated permittivity distribution can also be regarded as the discrete form of the forward problem:

$$\Delta C = J\Delta\varepsilon \tag{2}$$

where ΔC is the change of the measured capacitance, J is the Jacobian matrix, also known as sensitivity matrix and $\Delta\varepsilon$ can be regarded as a perturbation of the permittivity.

In multi-frequency TD imaging, excitation voltages with multiple frequencies are applied across the sensor. At time t_0, the measured capacitance is recorded as C_{t0} and it is taken as the reference value. Then, the measured capacitance at time t_1 is recorded as C_{t1} and the capacitance change with respect to C_{t0} is used for the permittivity distribution calculation, which is calculated by:

$$\Delta C = C_{t1} - C_{t0} \tag{3}$$

In this work, we propose the FD imaging of CVECT, where excitation voltages with different frequency components, i.e., f_1, f_2, f_3 ... f_l, are applied across the ECT electrodes and each excitation frequency corresponds to a measured capacitance value. Then, the relative measured capacitance difference is chosen to achieve the image reconstruction process. So, in FD imaging, the capacitance difference is calculated by:

$$\Delta C = C_{f1} - C_{f0} \tag{4}$$

When ΔC is obtained, the inverse problem of ECT is to determine the permittivity distribution from the capacitance measurement. Because the calculated permittivity distribution is usually demonstrated as a visual image, the inverse problem can be regarded as an image reconstruction process as well.

Algorithms for solving the ECT inverse problem include non-iteration and iteration algorithms. The former includes linear back-projection, direct method based on singular value decomposition, Tikhonov regularization [6], and other algorithms [1]. The latter contains the Newton–Raphson method, Landweber iteration, algebraic reconstruction technique and other related algorithms [1].

From the equation above, we found that both the forward model and inverse solver describe a relationship between the measured capacitance and the permittivity distribution. However, the performance of conventional ECT system is not ideal when the background conductivity increases and it usually does not work under a highly conductive background. Meanwhile, the excitation signal for typical ECT is single frequency, which means that the permittivity distribution calculation is limited to a certain range.

B. Multi-frequency complex-valued ECT

The complex-valued ECT (CVECT) has been reported in recent years [5]. Both permittivity and conductivity distribution can be calculated simultaneously by implementing CVECT and the excitation signal is multi-frequency.

The sensitivity matrix of CVECT is calculated based on the fundamental perturbation theory [5] and can be written as :

$$J = \frac{\partial C_c}{\partial E_{real}} \quad or \quad \frac{\partial C_c}{\partial E_{imaginary}} \tag{5}$$

where C_c is the measured complex capacitance value.

Therefore, by substituting (5) into (2) and performing a simple mathematical manipulation, (2) can be re-written into complex form:

$$\Delta C_{complex} = J_{complex}\Delta\varepsilon_{complex} \tag{6}$$

where $C_{complex} = \frac{Y}{i\omega}$ and Y is the complex admittance.

By simply manipulating (6), it can be expressed in the matrix format as below:

$$\begin{bmatrix} J_{r,\varepsilon} & J_{r,\sigma} \\ J_{i,\varepsilon} & J_{i,\sigma} \end{bmatrix} \begin{bmatrix} \Delta\varepsilon_r \\ \Delta\varepsilon_i \end{bmatrix} = \begin{bmatrix} \Delta C_r \\ \Delta C_i \end{bmatrix} \tag{7}$$

where the subscript "r" represents the real part and "i" stands for the imaginary part. ε_r is the real part of the complex permittivity distribution and it is a real permittivity value; ε_i as the imaginary part of $\varepsilon_{complex}$, it is calculated from conductivity and angular frequency, which is $\frac{\sigma(x)}{\omega}$.

Equation (7) describes the forward problem for CVECT. To solve the inverse problem of CVECT, a novel method to achieve image reconstruction will be illustrated in Section II-C.

C. Image reconsturction for CVECT

In previous study, the reported image reconstruction for CVECT was mainly based on Tikhonov regularization algorithm.

To be more straightforward, (7) can be formulated as:

$$\mathbf{C} = \mathbf{SG} \tag{8}$$

where $\mathbf{C} = \begin{bmatrix} \Delta C_r \\ \Delta C_i \end{bmatrix} \in \mathbb{R}^{m \times 1}$, $\mathbf{S} = \begin{bmatrix} J_{r,\varepsilon} & J_{r,\sigma} \\ J_{i,\varepsilon} & J_{i,\sigma} \end{bmatrix} \in \mathbb{R}^{m \times n}$ and $\mathbf{G} = \begin{bmatrix} \Delta\varepsilon_r \\ \Delta\varepsilon_i \end{bmatrix} \in \mathbb{R}^{n \times 1}$.

In general, according to (8), the perturbation of complex permittivity in $\mathbf{G}$ can be obtained by solving the following constrained optimization problem:

$$\begin{cases} \underbrace{min}_{\mathbf{G}} \quad R(\mathbf{G}) \\ s.t. \quad \mathbf{SG} = \mathbf{C} \end{cases} \tag{9}$$

where R is the regularization function.

Existing work has implemented the Tikhonov regularization algorithm for CVECT to achieve the image reconstruction process [5] and can be formulated as:

$$\begin{cases} \underbrace{min}_{\mathbf{G}} \quad ||\mathbf{G}||_2^2 \\ s.t. \quad \mathbf{SG} = \mathbf{C} \end{cases} \tag{10}$$

However, the Tikhonov regularization algorithm is a high computational cost algorithm because it can only achieve the image reconstruction step by step in the multi-frequency excitation scenario.

D. Proposed MMV method

Instead of applying the traditional algorithms, the MMV method is implemented to simultaneously and efficiently reconstruct images based on complex capacitance measurement. Since under different excitation frequencies, the pixels at the same position in each image have strong correlation with each other. Therefore, such correlation can be used as prior knowledge during the image reconstruction process.

According to (8), the MMV method for FD imaging can be formulated as:

$$\begin{bmatrix} \mathbf{C_{f1}} \\ \mathbf{C_{f2}} \\ \vdots \\ \mathbf{C_{fl}} \end{bmatrix} = \begin{bmatrix} \mathbf{S_{f1}} & & & \\ & \mathbf{S_{f2}} & & \\ & & \ddots & \\ & & & \mathbf{S_{fl}} \end{bmatrix} \begin{bmatrix} \mathbf{G_{f1}} \\ \mathbf{G_{f2}} \\ \vdots \\ \mathbf{G_{fl}} \end{bmatrix} \tag{11}$$

where $\mathbf{C_{fi}}$, $\mathbf{S_{fi}}$ and $\mathbf{G_{fi}}$ with $i = 1, 2, 3...l$ are the collection of measured complex capacitance, Jacobian matrix, and calculated complex permittivity under excitation voltage with l different frequencies, respectively.

The objective of the MMV method is to obtain the best solution of a collection of complex permittivity $\mathbf{G}$ with the know values of measured complex capacitance $\mathbf{C}$ and the given Jacobian matrix $\mathbf{S}$. For simplicity, (11) can be expressed as:

$$\tilde{\mathbf{S}}\tilde{\mathbf{G}} = \tilde{\mathbf{C}} \tag{12}$$

Therefore, the complex permittivity change distribution within the detecting region can be estimated by solving the following weighted optimization problem with certain constraints:

$$\begin{cases} \underbrace{\min}_{\mathbf{G}} \left\|\tilde{\mathbf{G}}\right\|_{w,2,1} = \sum_{i=1}^{nl} w_i \left\|\tilde{\mathbf{G}}_{b_i}\right\|_2 \\ \qquad \text{s.t.} \quad \tilde{\mathbf{S}}\tilde{\mathbf{G}} = \tilde{\mathbf{C}} \end{cases} \tag{13}$$

where w is a weighting factor and $\tilde{\mathbf{G}}_{b_i}$ denotes the subvector of $\tilde{\mathbf{G}}$ indexed by b_i. Generally, any index sets can be given by b_i.

Equation (13) is actually a group sparse optimization with weighted $l_{2,1}$-regularization problem [7]. The alternating direction method of multipliers (ADMM) method [8] is chosen to solve the optimization problem described in (13).

III. Results and Discussion

Numerical results are illustrated in detail in this section. FD imaging of CVECT using MMV model is comprehensively evaluated using simulation data. The performance of the proposed method is compared with that of the conventional Tikhonov regularization algorithm.

A. Phantom

Fig. 1 presents the simulated phantom to be imaged. An eight-electrode ECT sensor was employed. The outside and

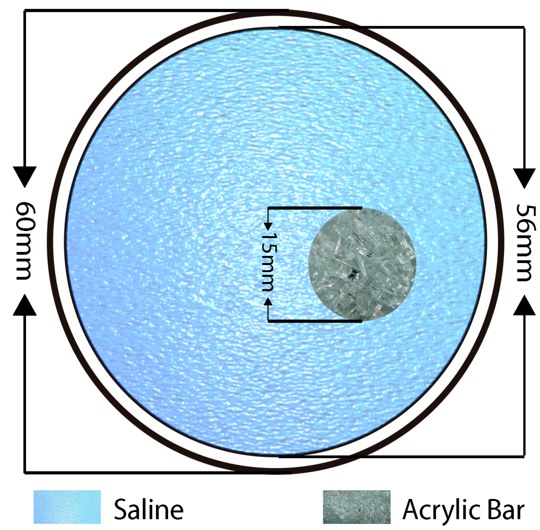

Fig. 1. *Top view of the eight-electrode CVECT phantom and detecting material includes saline with conductivity at 0.2 S/m and one acrylic bar with diameter at 15mm.*

inside diameters of the sensor are 60 and 56 mm, respectively. The background of the phantom is saline with conductivity of 0.2 S/m. An acrylic bar with a diameter of 15 mm is placed within the imaging region of the ECT sensor.

Fig. 2 demonstrates the perspective view of the ECT sensor in simulation by implementing COMSOL software. Eight-electrode CVECT censors are uniformly installed around the tube and detecting area is the inside circle of the tube. The measured complex capacitance data will be transferred, collected, analysed in MATLAB 2018b.

B. Simulation setup

In simulation, the phantom is simulated with the background conductivity set as 0.2 S/m. When implementing the MMV and Tikhonov regularization algorithm, the maximum iteration number is set as 800 and the stopping tolerance is chosen to be 1e-10. The iteration process will stop if it meets either condition.

For the phantom FD imaging, four excitation frequencies, 2.6 MHz, 3.8 MHz, 4.7 MHz and 5.6 MHz are selected with

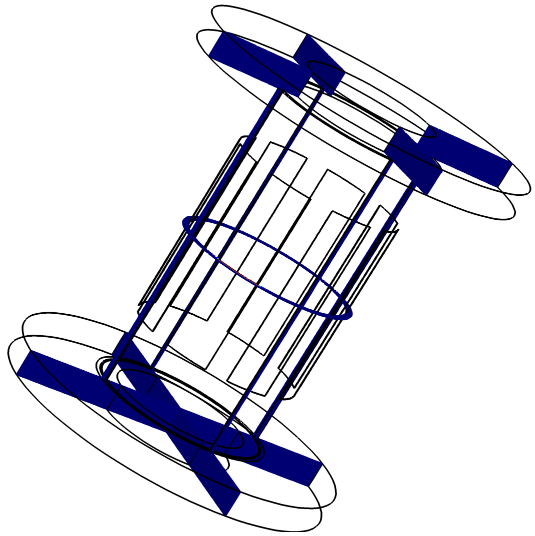

Fig. 2. *Eight-electrode ECT sensor model in COMSOL Multiphysics*

reference frequency at 2.0 MHz. The sensing strategy is the same as the typical ECT sensing strategy, which is reported in [1]. With eight-electrode ECT system, 28 non-redundant measurements are obtained.

C. FD imaging results

In this section, the image reconstruction results using Tikhonov regularization and MMV method are presented. As demonstrated in the first column of Table I, four excitation frequencies were imaged with reference frequency at 2.0 MHz and background conductivity at 0.2 S/m. Table I illustrates the permittivity and conductivity distribution reconstruction results of the phantom within the given frequency range.

The conductivity distribution can be well reconstructed for both algorithms except that no information at 2.0 MHz, which is the reference excitation frequency. According to (4), the difference of the measured complex capacitance should be zero at reference frequency and so the complex permittivity distribution cannot be obtained. However, for other three frequencies, the MMV method has a much better reconstruction quality of permittivity distribution than the conventional Tikhonov regularization algorithm.

In addition, previous work reveals that for TD imaging under 6.25 MHz, noise significantly affects the quality of complex permittivity distribution reconstruction and leads to failure of the reconstruction process for the Tikhonov regularization algorithm. Under noise free condition, Tikhonov algorithm is able to reconstruct images with considerable quality in a large frequency range [9]. In FD imaging, obviously, the results in Table I prove that the MMV method performs more stably than the Tikhonov regularization algorithm in a wide frequency range scenario and can achieve a much better reconstructed permittivity image quality under noise free condition.

To compare the efficiency, two algorithms were implemented and ran in MATLAB 2018b with same condition. The results shown that it took around 0.48 seconds and 0.85 seconds for MMV and Tikhonov regularization algorithms to reconstruct images, respectively. The findings prove that MMV is a more efficient method in image reconstruction than Tikhonov algorithm.

In summary, the simulated FD imaging results confirm that a reliable performance of CVECT system can be achieved. High-quality tomographic images can be expected by using the MMV method with high efficiency. Therefore, the MMV based FD imaging for CVECT method has potential applications where taking a reference measurement is not practical.

IV. CONCLUSION

In this paper, FD imaging as a novel data collection scheme and MMV image reconstruction framework for multi-frequency CVECT system were proposed. The FD-CVECT image reconstruction problem is expressed as a weighted $l_{2,1}$ norm minimisation problem and solved by implementing ADMM method. The feasibility of FD-CVECT has been verified, and its performance was evaluated based on simulation data. Compared with TD imaging method, FD imaging does not require a reference to be taken and thus is more promising in complicated scenarios where obtaining a reference is not possible. The proposed MMV model can reconstruct simultaneously multi-frequency images by considering the fact that images under different frequencies exist strong correlations with each other. Such correlations can be used as a priori information for enhancing image quality. The results of this work indicated that MMV model is able to reconstruct images with higher image quality compared with the conventional Tikhonov regularization algorithm. The combination of FD imaging and MMV model in CVECT has demonstrated huge potential for multiphase flow measurement, especially for flows containing highly conductive medium such as saline.

Future work will investigate the performance of FD CVECT for complex impedance distributions and relative experiments will be performed to further validate the results in this paper.

REFERENCES

[1] W. Yang and L. Peng, "Image reconstruction algorithms for electrical capacitance tomography," *Measurement science and technology*, vol. 14, no. 1, p. R1, 2002.

[2] Y. Liu, Y. Deng, M. Zhang, P. Yu, and Y. Li, "Experimental measurement of oil–water two-phase flow by data fusion of electrical tomography sensors and venturi tube," *Measurement Science and Technology*, vol. 28, no. 9, p. 095301, 2017.

[3] T. Dyakowski, G. A. Johansen, B. T. Hjertaker, D. Sankowski, V. Mosorov, and J. Wlodarczyk, "A dual modality tomography system for imaging gas/solids flows," *Particle & Particle Systems Characterization*, vol. 23, no. 3-4, pp. 260–265, 2006.

[4] J. A. Fracassi da Silva and C. L. do Lago, "An oscillometric detector for capillary electrophoresis," *Analytical Chemistry*, vol. 70, no. 20, pp. 4339–4343, 1998.

TABLE I
FD IMAGE RECONSTRUCTION OF PHANTOM 1 WITH BACKGROUND CONDUCTIVITY AT 0.2 S/M

Frequency (MHz)	Tikhonov Regularization		MMV	
	$\Delta\varepsilon$	$\Delta\sigma$	$\Delta\varepsilon$	$\Delta\sigma$
2.0	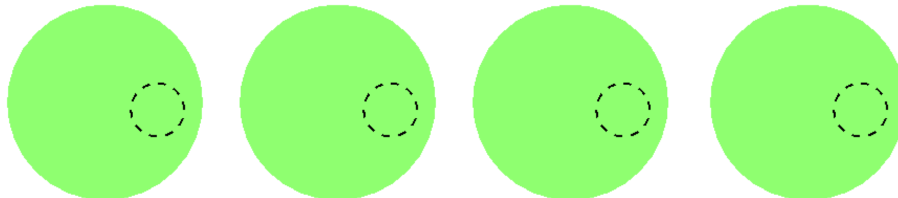			
2.6	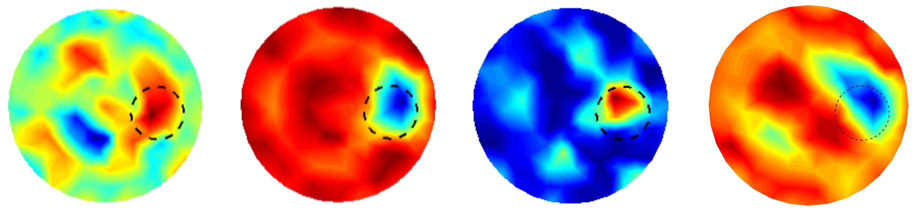			
3.8	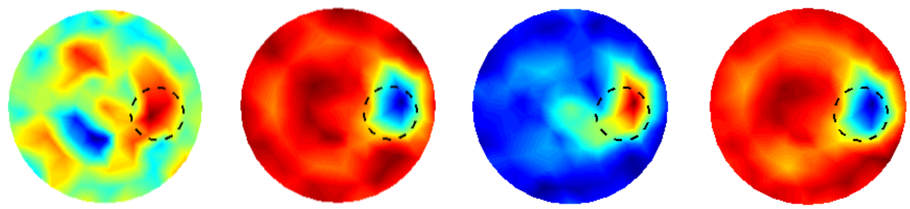			
4.7	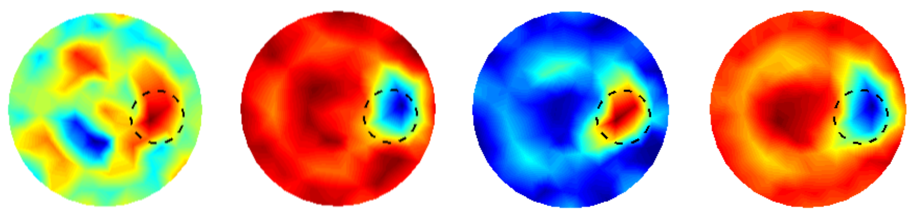			
5.6	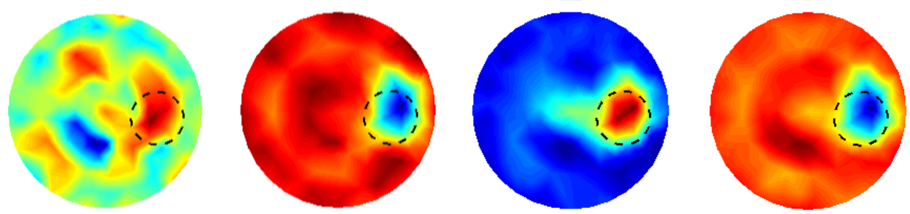			
Colour bar	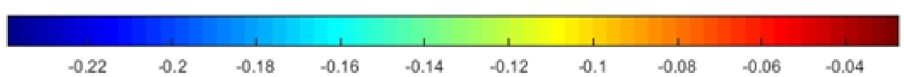			

[5] M. Zhang and M. Soleimani, "Simultaneous reconstruction of permittivity and conductivity using multi-frequency admittance measurement in electrical capacitance tomography," *Measurement Science and Technology*, vol. 27, no. 2, p. 025405, 2016.

[6] A. N. Tikhonov and V. I. Arsenin, *Solutions of ill-posed problems*. Winston, Washington, DC, 1977, vol. 14.

[7] Y. Yang, H. Wu, and J. Jia, "Image reconstruction for electrical impedance tomography using enhanced adaptive group sparsity with total variation," *IEEE Sensors Journal*, vol. 17, no. 17, pp. 5589–5598, 2017.

[8] W. Deng, W. Yin, and Y. Zhang, "Group sparse optimization by alternating direction method," in *Wavelets and Sparsity XV*, vol. 8858. International Society for Optics and Photonics, 2013, p. 88580R.

[9] M. Zhang, Y. Li, and M. Soleimani, "Experimental study of complex-valued ect," in *9th World Congress in industrial process tomography, WCIPT9, Sep 2018*, 2018.